Model-based Interpretation of Anatomical Structures in Cranial MR Images

C I Attwood[†], G D Sullivan[†], G P Robinson[‡], K D Baker[†] and A C F Colchester[‡]

[†]Dept of Computer Science, University of Reading

[‡]Dept of Neurology, UMDS, Guy's Hospital

A symbolic model of cerebral anatomy is outlined. Rules based on a multi-resolution representation of MR images, are used to instantiate principal landmarks in the model. These then allow a more detailed analysis of image features, using the expected structure of secondary anatomical features.

INTRODUCTION

This paper reports work carried out within the Alvey MMI-134 project ("Model-based Interpretation of Radiological Images"). The objective of the work is to identify and label the anatomical structures visible in multi-slice Magnetic Resonance (MR) Images of the head. An example image is shown in Figure 1.

The identification of anatomical structures requires:

(1) A means to represent the anatomical knowledge which defines the structures.

(2) A representation of the image data, which allows important features to be extracted easily.

(3) A set of recognition rules, allowing features found in (2) to be identified with objects in (1).

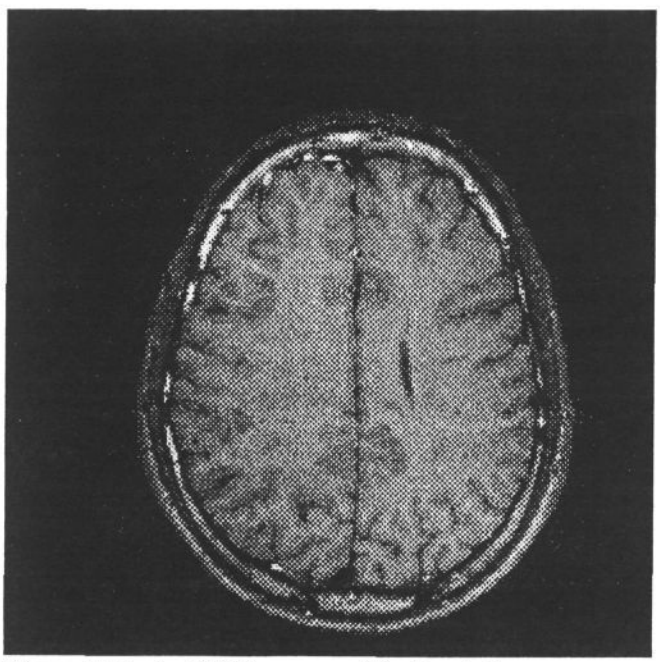

Figure 1. Typical MR image used in the study.

Anatomical structures are inherently difficult to encode, since there is considerable variation between different patients. Furthermore, the image detail is greatly affected by the control settings of the imager, and the geometry of the slice.

A hierarchical model of the brain has been developed, based on the ART™ system, in which nodes represent the structures of interest, and arcs represent 3-D topographical relationships between organs and part-of relationships. The nodes contain attributes of the organs which encode their expected shape and identifying features; they also attach to the recognition rules, which use the measured attributes and relationships to identify the structures.

In this paper the image data is pre-processed to create a Laplacian Pyramid by using multiple Difference of Gaussian (DoG) filters (see Figure 2). Most of the reasoning used in the recognition rules is based on zero crossing features of the DoG images, which may be tracked between scales, or between images of adjacent slices.

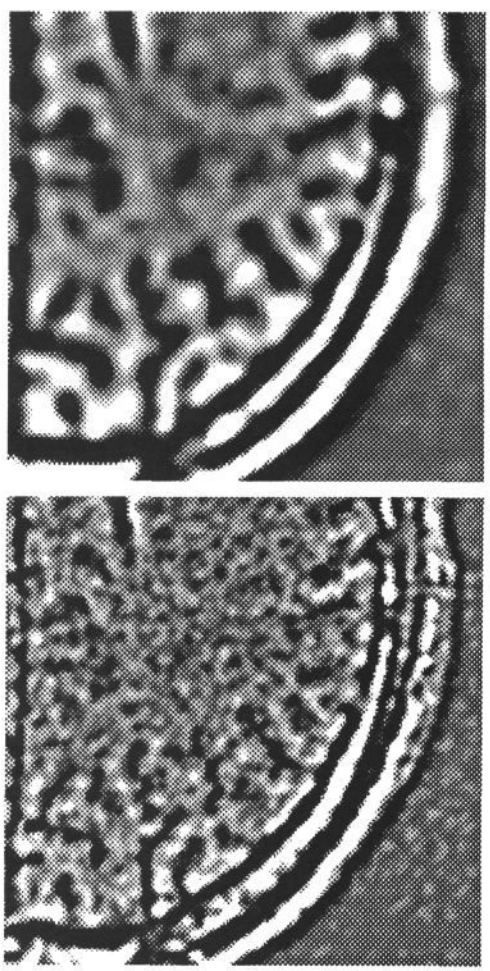

Figure 2. DoG images at 2 scales, of the lower portion of figure 1.

BMVC 1990 doi:10.5244/C.4.27

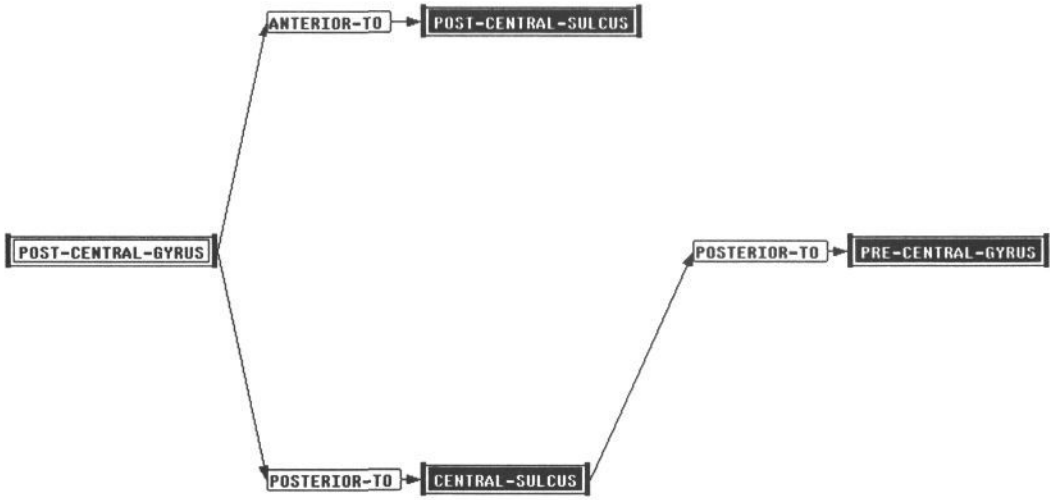

Figure 3. Fragment of the symbolic anatomical model, showing typical spatial relationships.

Other features of DoG images, such as ridges, and the statistics of lobes in them, or indeed other image coding schemes (Rosin et al 1990) are also under study within the Alvey project.

This paper mainly concerns the anatomical model, and the recognition rules based on features in the DoG data set. Principal landmarks such as the scalp outline, and the lateral ventricles can be identified with the minimum of contextual knowledge. The anatomical model then mobilises detailed expectations whereby context-specific knowledge can be used to search for less well-defined organs. This in turn further instantiates the model and the final interpretation evolves progressively.

THE ANATOMICAL MODEL

Essential anatomical facts are represented by means of a high level symbolic model of the human brain. This model takes the form of a frame-based semantic network, which is complementary to other low-level models (Niemann et al (1988), Mowforth & Zhengping(1989), Hawkes et al (1990)). The nodes in the network represent anatomical features. Links in the network express spatial and logical relationships between the anatomical features. The model can be viewed conceptually as three co-existing graphs. The first represents a part hierarchy describing the required components of the brain. The second is a graph of adjacencies or constraint relations between nodes in the model. For most anatomical features the spatial relations are expressed only between

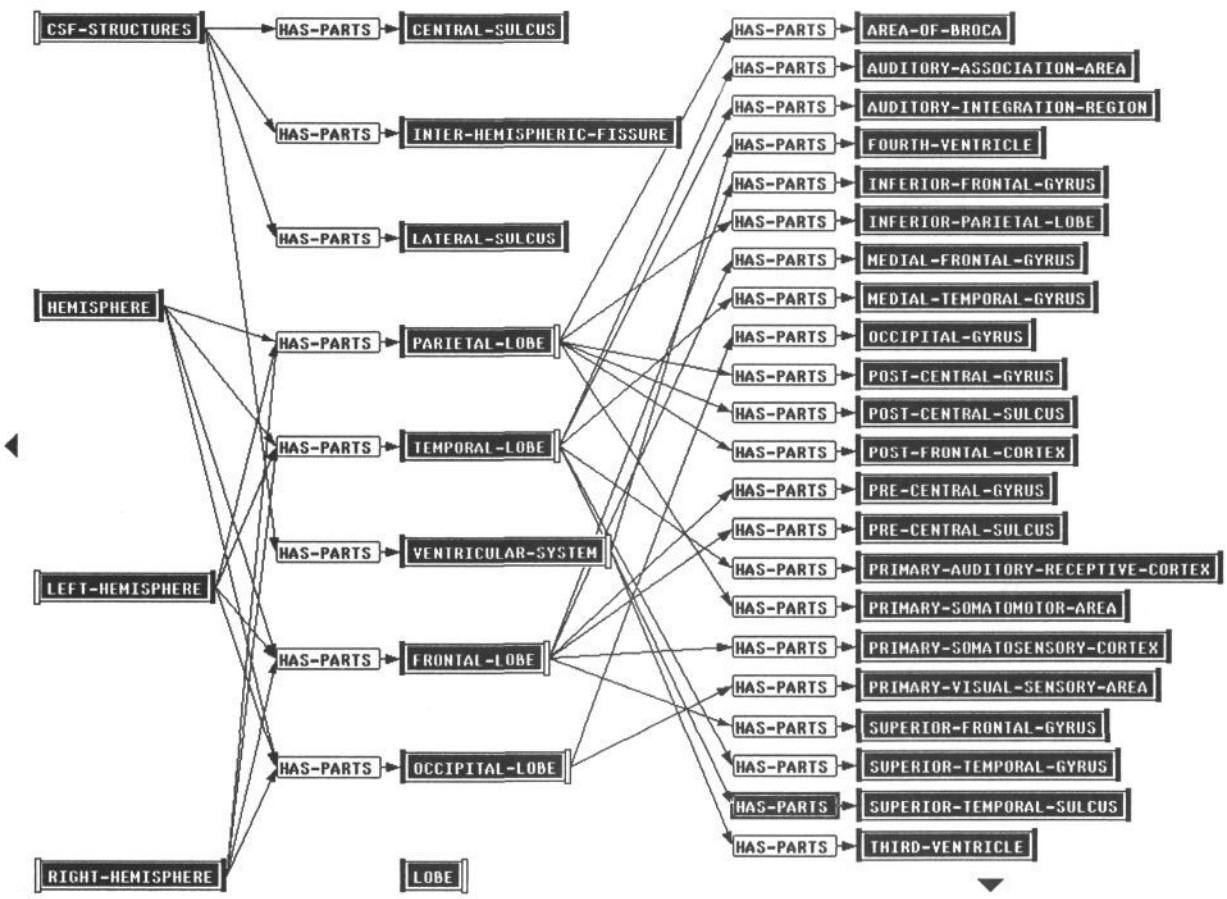

Figure 4. Part of the anatomical model.

nodes at the same level in the part hierarchy. Spatial relationships between nodes at different levels can be inferred. The third graph is an IS-A type graph connecting image features to the model.

Salient features in the image are located and summarized in terms of their position and shape. These initial features are then labelled as candidate nodes in the model allowing for one image feature to be a candidate for many nodes. Initial matching between nodes in the model and image features is based on intrinsic attributes of features such as size and shape (as opposed to relationships between features). Multiple 'viewpoints' are used to allow the co-existence of potentially conflicting hypotheses. For example, the hypothesis that feature "A" extracted from the input image is an inferior horn of the left lateral ventricle is conflicting with the hypothesis that "A" is an inferior horn of the right lateral ventricle. Even so, both hypotheses may be supported to the same degree and both must be allowed to co-exist.

The 'model viewpoint' contains all the information regarding the anatomical model (Figure 3 & 4), as well as rules for combining and reasoning about viewpoints. New viewpoints are generated whenever a potential image feature has been located in the images and a label assigned to a model node.

Merging of viewpoints is controlled via a rule base which decides whether salient features are compatible with each other. If viewpoints are not incompatible, then they are merged and replaced by a new viewpoint. This creates a tree structure of co-existing viewpoints.

Further processing is carried out to support or refute viewpoints until the number of remaining viewpoints can no longer be reduced. The result of further processing may be to 'poison' viewpoints as well as to merge them. Compatibility of viewpoints is checked by comparing spatial relationships between nodes in the model with spatial relationships between image features. For example if an image feature "A" is labelled as the 'post-central-gyrus' and a second image feature "B" is labelled as the 'central-sulcus', then "A" must be posterior-to "B" as this is a pre-requisite specified in the anatomical model. If "A" and "B" are not compatible then no hypothesis is allowed to exist in which they are both true.

Figure 2 shows a stylized view of the part of the knowledge base used in the location and identification of the major sulci and gyri on the cortical surface.

IMAGE DESCRIPTIONS

MR images were acquired with a 1.5 Tesla Phillips Gyroscan, using a T1 weighted spin-echo pulse sequence with two signal averages; producing 126 slices at 256X256 resolution. DoG filters of either 1/2 or 1 octave separation have been used depending on the quality of the image set. The notation used in this paper, for example, $DoG_{8\text{-}16}$ refers to a filter comprising a +ve Gaussian of $\sigma_1 = 8$ and a -ve of $\sigma_2 = 16$.

The shape of image features is extracted in the form of a skeleton description, or as edge-contours taken from DoG images. These are the primary features which are matched against objects held within the model.

Figure 2 illustrates the fact that the evidence for anatomical structures in the DoG images is highly dependent on the scale used: coarse scales are simple but inaccurate, fine scales are detailed, but confused. Different scales are useful for different aspects of the visual interpretation process. The initial localisation and identification of the most conspicuous organs can often be carried out in coarse scales. This estimate provides a context which can then be used to seed a search for more accurate location in finer scales (details are given in the Appendix).

The recognition rules in this work use two primary features derived from DoG images: the binarised regions of connected positive or negative values (dark and bright lobes in Figure 2), and the connected contours formed by the ZCs. The main attributes computed include the position in the image (relative to the outer boundary of the scalp), shape characteristics of the zero crossing contours, first and second order statistical measures of the regions, and characteristics of the symmetry axis transforms of the regions. Two types of features, and their corresponding recognition rules have been implemented: region-based, and edge-based.

Region-based methods. Binarised DoG images (see Figure 2) are segmented into connected components to form separate regions. A wide range of conventional region-based measures can be applied. We make use of the low-order statistics, and also the position, structure and curvature of the symmetry axis transforms (derived either by maximal disc, or grass-fire algorithms, Arcelli (1981)).

Manually identified regions in trial images have been used to establish prototypical attributes for some of the major anatomical structures, including the scalp outline, the sub-arachnoid space, and the body and posterior horn of the lateral ventricles.

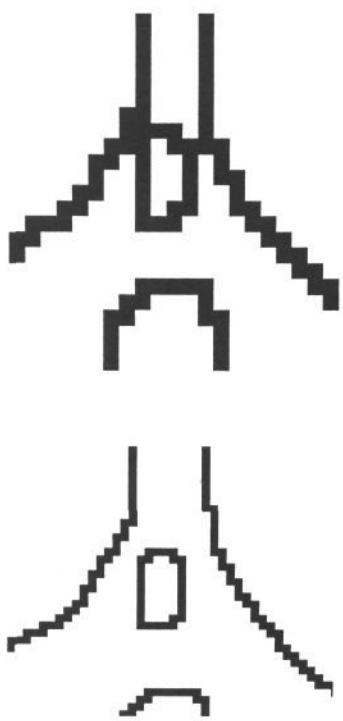

Figure 5. Zero-crossing connectivity confusions avoided by bi-linear pre-scaling of the image.

Edge-based methods. Zero-crossings (ZC) in the DoG images are connected into contours by tracking between neighbours. One attraction of using ZCs is that, in principle, they form distinct closed contours. However, two problems arise in practise with discretely sampled images: i) locally ambiguous

connections, where ZCs touch, and ii) disruption by noise. These problems can often be controlled by applying a threshold based on the ZCs slope when extracting connected contours, and then connecting nearby free-ends (which have the right polarity).

Zero-crossings are sampled at the pixel density. Therefore local ambiguity of connectivity is frequently observed at the finest scales used (see Figure 5) because independent ZCs can occur in adjacent pixels. Hildreth's algorithm overcomes this by modeling the ZCs to sub-pixel accuracy. We have adopted a simpler method. The image is first expanded by bi-linear interpolation, then the DoG filter is applied (at twice the scale). This proves to be very effective in disambiguating the connectivity in ZCs (see Figure 5).

RECOGNITION RULES

Simple characteristics in a coarse scale image ($DoG_{8\text{-}16}$) may be used to identify the principle landmarks in the image. The landmarks then focus subsequent search for other detail. The following methods have been developed.

(1) Identification of the scalp outline. The outer scalp boundary is usually very easy to identify in an MR image such as Figure 1. The ZC contours in an intermediate scale usually contains a strong outermost curve of appropriate polarity. Subject to certain rules for expected size (given the approximate position of the slice), and position this is accepted as the scalp outline.

The scalp outline is normalised (by radial expansion) to a unit circle, and this provides the coordinate frame for further processing (the orientation remains that of the original image).

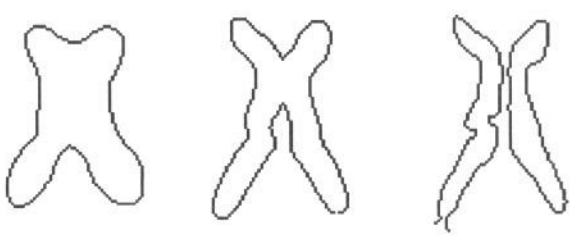

Figure 6. Coarse-to-fine refinement of the lateral ventricles.

(2) Identification of the ventricles. The ventricles are often very well defined, and have good contrast in the images. A search is carried out in a coarse scale of DoG for centrally located lobes of appropriate size and polarity. Candidate contours are tested for simple symmetry with respect to the vertical axis. Any found, are used to seed a coarse-to-fine track (see Appendix) through successively finer ZC images (Figure 6).

This cue is fairly robust against scale, and in our experience to date any mid-range filter can be used.

(3) *Identification of the cortical surface.* Preliminary experiments showed that the cortical surface is usually associated with ZCs in $DoG_{4\text{-}5.6}$ scale images.The local-connected ZCs from the DoG are first normalised relative to the scalp outline (this causes the cortical surface, to lie at a roughly constant distance from the scalp centre). Lines lying at least partly within a radius of between 0.7-0.9 units in the normalised coordinate system are extracted as candidates for the cortical surface. Large lines are extracted and low radius breaks joined up if they are unambiguous. The resulting set of lines is compared on a number of criteria, including size, centre of gravity relative to the scalp centre, and simple topological relationships.

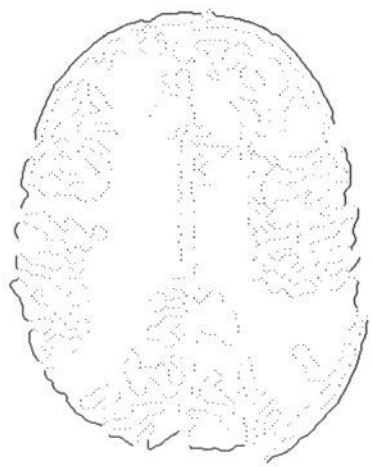

Figure 7. Example of cortical boundary, as traced by the ZCs; regions labeled as gyri are shown darker and sulci lighter.

The cortex appears as two separate hemispheres in higher brain slices above the corpus callosum. This algorithm has proved robust enough to identify the cortical boundary in over 30 images from two sources.

(4) *Identification of the major sulci and gyri.* Having identified the cortical surface, the function $S(\theta)$ is calculated, where θ is the angle subtended at the scalp centre.

S is the value of the intrinsic parameter (the ordinal position along the connected contour) as a function of θ, at points on the contour furthest from the centre of the scalp. S varies continuously along the tangential parts of the cortical surface, indicating gyri. Where a concavity occurs, which might possibly indicate the presence of a sulcus, the S function changes abruptly. S is differentiated, and peaks above fixed-threshold are selected as candidate sulci. Conversely, the places where the S pointer runs in sequence are labeled as gyri, selected as the connected sequence lying between adjacent sulci. The position of a sulcus is given by the θ values of the end points of the discontinuities in S. Its extent is recovered as the connected line lying between pointers into the original cortex surface. Figure 8 shows an example of the recovered cortical description.

(5) Identification of the inter-hemispheric fissure. Sulci lying close to the mid-line of the scalp outline are taken as candidates for the inter-hemispheric fissure.

In experiments to date this has been unambiguous. The exact location and form of the fissure is localised more precisely, by tracking into finer scales using the same techniques used in refining ventricle positions (See Figure 9).

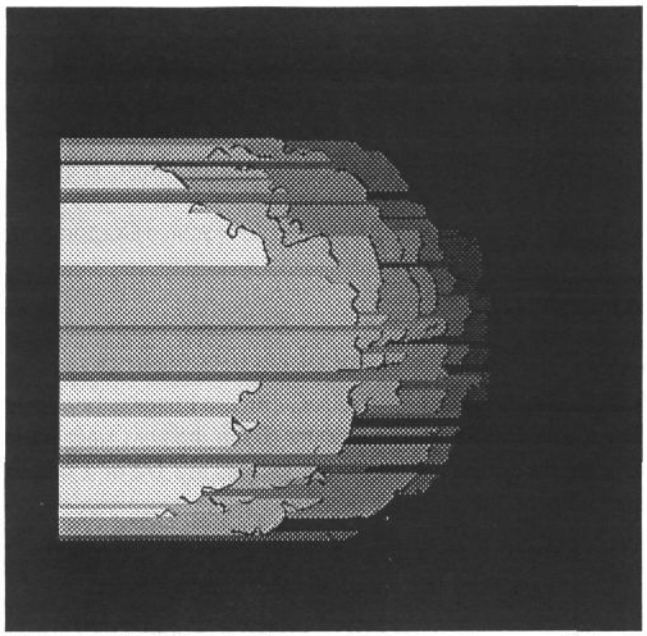

Figure 8. Right-hemisphere gyri recovered separately in 10 slices; note the regions labeled as sulci have been left as gaps, which are often consistent between slices.

MODEL INSTANTIATION

The identification of the major landmarks in the images establishes a coordinate frame for quantitative geometrical relationships, and allows a partial instantiation of the anatomical model. The emerging interpretation of the image makes it possible to seek further image details indicating anatomical structures which are less conspicuous, or whose geometry is more difficult to characterise.

The concavities in the line deemed to be the cortical surface provide initial estimates of the positions of the major sulci and gyri. Figure 10 represents a section of the hemisphere on the right of Figures 1 & 7, as if viewed from the right. The ordinate corresponds to 22 slices (from images spaced with 2 mm separation. The abscissa shows orientation around the brain centre, ±45 degrees around the right lateral axis. Each vertical bar show the position and extent of a sulcus as identified by the above recognition rules. In effect the diagram simulates a view of a piece of the cortical surface visible from the right, as it has been interpreted by the system.

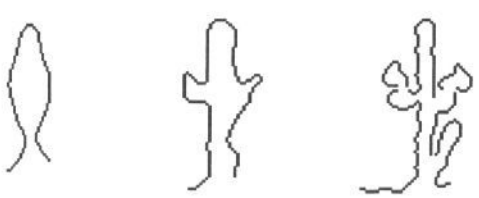

Figure 9. Coarse-to-fine tracking of the rear portion of the inter-hemispheric fissure.

There are obvious regularities in Figure 10. The "sulci" do tend to run in lines, and the gaps between sulci (gyri) do form coherent regions. However visual comparison with the original data shows that there are many errors. Sulci may be missed, usually due to a disconnection between ZCs which identified the cortical surface and the visible sulcus. Failures also arise due to the cortical line becoming attached to image features in the skull; this proved particularly troublesome in some slices. An example can be seen in Figure 7 where such an event occur at the top and bottom-right of the image. We believe that fairly simple improvements to the recognition rules will eliminate many of these errors. In particular the potential for using deformable models to overcome such problems is being studied (Karaolani et al (1989), Sullivan et al (1990)).

The identification of consistent runs of sulci in Figure 10 raises the problem of finding the correspondences between slices. Attributes of competing sulci, already available in the representation such as maximum depth, length and principal orientations, may be used as criteria for matching. The coarse-to-fine algorithm can also be adapted to correlate image features in adjacent slices.

Work is currently directed towards grouping together extended "sulcus" features, and to establish recognition rules which allow candidates for the major cortical features to be instantiated in the anatomical model.

On the supero-lateral part of the hemisphere, illustrated in Figure 3, the most reliable features are the pre-central gyrus, the central sulcus and the post-central gyrus. Candidate image features will be used to create hypothetical matches to model nodes, ie, new viewpoints. Viewpoints which can be combined so that topographical relationships between elements that are consistant with the model (see Figure 4) will survive. When the more distinctive model features have been matched to image features, attempts can be made to instantiate adjacent model elements by searching the parts of the image indicated by the topographical relationship coded in the model.

DISCUSSION

Experiment have been carried out on the use of multiple scales of analysis for locating and labelling cerebral structures. The most conspicuous features - such as the scalp and the ventricles can successfully be found, using fairly simple context-free feature-extraction methods, combined with simple recognition rules. These landmarks are used to instantiate a symbolic anatomical model. This makes available higher-level knowledge to assist further image processing. The rules rely on specialised heuristics and opportunistic reasoning.

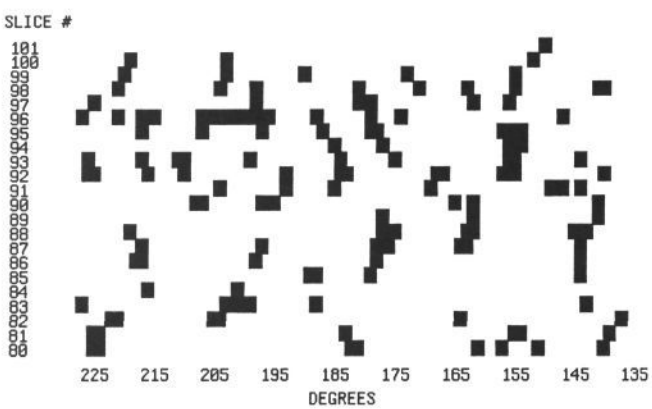

Figure 10. The position and angular extent of the cortical sulci recovered from a sequence of 22 MR images, shown in the form of a side view of the "unfolded" cortical surface.

This task domain of MR cranial images is particularly difficult for a number of reasons, especially the variety of shapes of the cortex within 'normal' brains. The delineation of the soft tissue from the surrounding cerebral-spinal fluid (CSF), scalp, fat and bone also presents significant problems. It is fairly common practice to outline the structures in such images by hand. However this operation is very poorly controlled, since it is difficult for the human operator to maintain a consistent criterion for the task. The use of high level anatomical models makes possible computer assistance in this process and in time may allow autonomous interpretation of medical images, and the registration of images from different modalities.

The use of DoG images is convenient, but non-ideal. High-contrast contours can reliably be found as ZCs in well-chosen scales, and these can then be tracked into finer scales (see Appendix). However, structures such as the cortical folds have compound edges, as two grey-matter "sheets" come into contact with each other, sometimes with traces of darker CSF in between. This information is not well represented in any single scale DoG. The image information is however present and can easily be reconstructed from DoG images (Sullivan & Baker, 1980) but richer representations of the image using hierarchical descriptions may be required (Rosin et al, 1990).

REFERENCES

Arcelli, C. "Pattern thinning by contour tracing". *Comp. Graph. & Im. Proc.* 17, pp. 130-144 (1981).

Hawkes, D.J. Hill, D.L.G. Lehmann, E.D. Robinson, G.P. Maisey, M.N & Colchester, A.C.F. "Preliminary Work on the Interpretation of SPECT Images with the Aid of Registered MR Images and an MR Derived 3D Neuro-anatomical Atlas". *3D Imaging in Medicine: Algorithms, Systems, Applications.* pp.241-251. (Ed: Höne, K.H. Fuchs, H. & Pizer, S.M., Springer-Verlag, (1990)

Karaolani, P. Sullivan, G.D. Baker, K.D. & Baines, M.J. "A Finite Element Method for Deformable Models". *Proc. 5th. Alvey Vision Conf.* Univ. of. Reading. England. (1989).

Mowforth, P.H. & Zhengping, J. "Model-based Tissue Differentiation in MR Brain Images". *Proc. 5th. Alvey Vision Conf.* Univ. of. Reading. England. (1989).

Niemann, K. Keyserlingk, D.G. & Wasel, J. "Superimposition of an Average Three-dimensional pattern of Brain Structure on CT scans". *Acta. Neurochirurgica*, 93, pp. 61-67, (1988).

Rosin, P.L. Colchester, A.C.F. & Hawkes, D.J. "Early Visual Representation Using Regions Defined By Maximum Gradient Profiles Between Singular Points". *I.P.M.I, Proc. X1th. Int. Meeting,* Berkeley, Calif. (D. Ortendahl, ed), Wiley: New York. (1990).

Sullivan, G.D. & Baker, K.D. "Multiple Bandpass Filters in Image Processing".IEE Proc.127(E),pp.173-184, (1980).

Sullivan, G.D. Worrall, A.D. Hockney, R.W. & Baker, K.D. "Active Contours in Medical Image Processing using a Networked SIMD Array Processor" Proc. BMVC Oxford, England (1990) (These proceedings).

Acknowledgments

This research was supported by Alvey project MMI-134 "Model-based Interpretation of Radiological Images". We would also like to thank the following for their help in this work; Guy's Hospital MR Unit, M. Graves & D. Hawkes.

APPENDIX

Coarse-to-fine tracking of zero-crossings

A connected contour (A) in a DoG-filtered image at one scale (D_1) is related to a set of contours (B) in the next finer scale (D_2), by the following algorithm (Scales are 1/2 or 1 octave apart, dependant on image quality).

(1) Expand A by a disc of radius $1.4\sigma_1$ (where $\sigma_1$is the value of the +ve sigma in D_2), to form a mask.

(2) Find all contours in D_2 intersecting with the mask (the set: I).

(3) Any curve in I which is closed is accepted in B

(4) Free ends on open contours in I are examined to complete loops which lie outside the mask. Free ends in I which can be connected in D_2 to a second free end in I (possibly the other end of the same contour) are identified. Any single contour in D_2 of length less than $3\sigma_1$ which links a pair of open ends in I is unioned with I.

(5) Steps 3 & 4 are repeated until stable, then all remaining contours in I are included in B.

Rule 4 allow loops to be completed, and contours to break into two closed forms (e.g. Figure 5).

The constants in rules 1 & 4 which control the mask width and permitted loop extensions have been determined empirically. They are related to the expected "slew" of an edge between scales, and the minimum curvature within a scale. Application specific heuristics must still be applied to cover the behaviour of ZCs in scalespace, for example, when tracking objects which are known to break into closed forms the $3\sigma_1$ criteria in rule 4 must be supplemented with another criteria; that a contour in D_2 that links ends in I but is greater than $3\sigma_1$ in length, may be used if it is interior to the boundary of A, i.e. the contour is splitting.